POLITECNICO
MILANO 1863

SCUOLA DI INGEGNERIA INDUSTRIALE
E DELL'INFORMAZIONE

Executive Summary of the Thesis

Exploring hybrid quantum-classical algorithms for calculating energy spectra of molecular aggregates

Laurea Magistrale in Materials and Nanotechnology Engineering - Ingegneria dei Materiali e delle Nanotecnologie

Author: Riccardo Ferrone

Advisor: Prof. Guglielmo Lanzani

Co-advisors: Prof. Cesare Soci, Dr. Anton Vetlugin (Nanyang Technological University Singapore)

Academic year: 2021-2022

1. Introduction

In this work, the application of quantum computers for investigating the optical properties of molecular aggregates has been investigated. The aim of this work is to evaluate the current performance of quantum computing and its ability to solve problems in quantum chemistry. Considering the current stage of quantum computing, hybrid quantum-classical eigensolvers have been exploited and tested using simulators of quantum processors as well as the real IBM quantum device. Simple systems of molecular aggregates were studied – a dimer (two-molecule system) and a tetramer (four-molecule system).

2. Theoretical background

2.1. Quantum computing

Quantum computing was firstly theorised by the physicist Richard Feynman in the 1980s. It refers to a fundamental shift in how computations are performed, by taking advantage of quantum physics unique properties. The main examples would be the possibility to exploit quantum entanglement to access a wider Hilbert space of possible solutions or the possibility to store information as a superposition of 0 and 1 states. Thanks to such characteristics quantum computer promise to solve classically intractable problems in many different fields spanning pharmacology, logistics, chemistry, and material science. For this reasons, many private and public entities started hugely investing in the field resulting in the first commercially available Quantum Processing Units (QPU) like the one employed in this work

Figure 1: IBM Q system one

As of today, quantum computing finds itself in

the so-called Noisy Intermediate-Scale Quantum (NISQ) era. Such term refers to quantum processors with low number of qubits, but enough not to be practically simulated by any classical computer, which are still prone to noise disruption. This means that the QPU wavefunction can be affected by the outside environment, leading to decoherence ("leakages" of small amount of information from the quantum system). The next step will be the introduction of Quantum Error Correction (QEC) codes to reduce or eliminate noise and allow the introduction of Fault-Tolerant Quantum Computers (FTQC) able to live up to the promises of quantum computing [1].

In quantum computers the information is stored in qubits (quantum bits), which allows to perform computation in the Hilbert space $\mathcal{H} = \mathbb{C}^{2^N}$, where N is the number of qubits. The state of a single qubit can be described as a vector in such Hilbert space:

$$|\Psi\rangle = \alpha\,|0\rangle + \beta\,|1\rangle$$
$$\text{where } \alpha, \beta \in \mathbb{C} \text{ and } |0\rangle = \begin{bmatrix}1\\0\end{bmatrix}, |1\rangle = \begin{bmatrix}0\\1\end{bmatrix} \quad (1)$$

The state of a qubit can be evolved to the desired one by applying quantum gates. Universal quantum computation can be implemented using single- and two-quabit gates. Single-qubit gates include X-,Y-, and Z-Pauli gates, Hadamard (H) and phase-shifting gates, as well as single qubit rotations R_x, R_y and R_z around the corresponding axes. Among two-qubit gates the CNOT (controlled-NOT) and the Toffoli gates are the most widely used. For instance, by combining H gate and CNOT gate, it is possible to entangle two qubits. Measurement of the qubit's state is performed by preparing the state multiple times and averaging the result.

Quantum computers can be used to perform simulations of quantum systems both for physics [2] as well as for chemistry applications [3]. Quantum simulations can be divided into three categories:

- **Analogue simulations**, where the interactions of a well controlled quantum system are engineered in order to reproduce the Hamiltonian of the system of interest.
- **Digital simulations**, where the wave function of the considered problem is encoded in the computational basis of the quantum computer, and Hamiltonian is decomposed into a sequence of quantum gates.
- **Digital-analogue simulations**, where large analog blocks are employed together with digital steps.

2.2. Molecular aggregates

Molecular aggregates are a specific set of materials composed by groups of molecules, usually dye molecules, held together by non-covalent forces. Molecular aggregates can be found in nature as well as made artificially. This class of material is characterised by peculiar optical proprieties which were firstly investigated by Michael Kasha et al. in the 1960s [4]. Specifically, the aggregation phenomena leads to a stark change in the absorption spectra from the monomeric one as a consequence of the interaction between molecular transition dipole moments. As a result, molecular aggregates are classified into two main groups: H-aggregates characterised by a blue-shifted band in the absorption spectra (Fig. 2a), and J-aggregate characterised instead by a red-shifted band in the absorption spectra (Fig. 2b).

This peculiar behaviour can be explained in first instance by employing the exciton model introduced by J. Frenkel in the 1930s [5]. Such model is based on the exciton quasi-particle, the bound state of an electron promoted to the conduction band and the corresponding hole in the valance band, which are attracted to each others by electrostatic forces. When a monomer composing a molecular aggregate is hit by radiation of the correct frequency a localised exciton arise with an associated transition dipole moment. The parallel alignment of the dipole moments results in the H-aggregate, while the in-line alignment produces the J-aggregate. In the simplest case of a dimer (two-molecule aggregate), the interaction between the dipole moments leads to a splitting of the degenerate energy spectra. The excited energy spectra for such small system can be easily computed analytically:

$$E_\pm = \epsilon \pm J, \quad (2)$$

where ϵ is the energy of the single excited molecule and J is the exciton splitting term defined as a Coulomb interaction according to the point-dipole approximation. As shown in Fig.

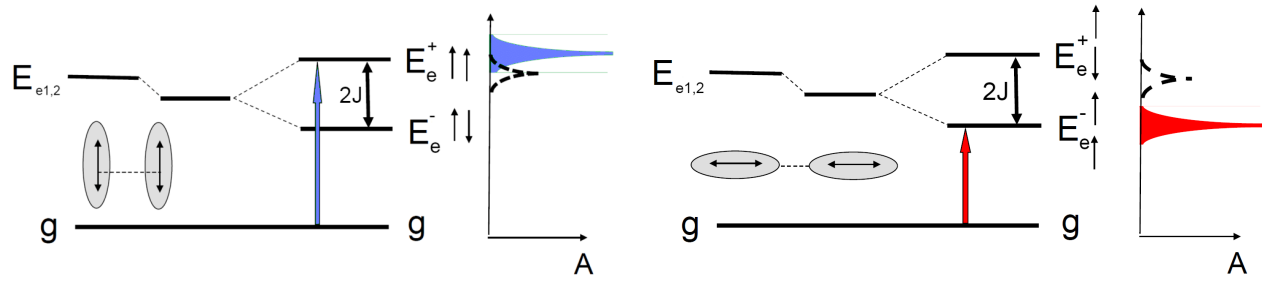

(a) H aggregate energy + optical spectra.

(b) J aggregate energy + optical spectra.

Figure 2: Schematic representation of the energy and optical spectra of H and J molecular aggregates.

2a and 2b the dimer transition dipole can be two times the monomer one or equal to zero according to whether the monomer dipole moments are in phase or out-of phase. The alignment of the monomers dipole moments determine also which of the two excited energy levels resulting from the splitting is the optically active one. This first simple but effective model based only on electronic excitation has been further elaborated in the past decades to encompass a more faithful description of the real systems. The latest theories developed allow to describe important proprieties such as J-band narrowing as well as exciton transport properties along molecular aggregates. This was achieved by considering in their description vibrational modes coupling with electronic transitions and the influence of the environment on the aggregate system.

3. Using quantum computing to simulate molecular aggregates

Investigation of molecular aggregates, including their photo-physical properties, is motivated by the important role they play in photosynthesis processes and artificial devices. Unfortunately, the current optical investigations techniques, i.e. far- and near-field optical spectroscopy, are not able to probe molecular aggregates spatial structure down to the single molecule level. This makes it difficult to study the effect of disorder and noise on exciton transport mechanisms and related photo-physical properties.

Beyond experimental difficulties, the properties of a molecular aggregate cannot be efficiently calculated using classical methods (many body problem). Here, the possibility of using quantum computers to facilitate simulation of molecular aggregates has been explored. Considering the current stage of quantum computing (NISQ), hybrid quantum-classical approaches have been implemented - the Variational Quantum Eigensolver (VQE) and the Variational Quantum Deflation (VQD) algorithm, where quantum and classical computation steps alternate.

3.1. Varitational Quantum Eigensolver (VQE) algorithm

Introduced by Peruzzo et al. [6], the VQE algorithm is a hybrid technique, which employs both quantum and classical resources in an iterative procedure in order to find the lowest energy eigenvalue. The VQE relies upon the Rayleigh-Ritz variational principle, according to which, for a parameterized trial wave function $|\Psi(\boldsymbol{\theta})\rangle$

$$\langle\Psi(\boldsymbol{\theta})|\, H\, |\Psi(\boldsymbol{\theta})\rangle \geq E_0, \tag{3}$$

where E_0 is the lowest energy eigenvalue of the Hamiltonian H (the Hamiltonian of the analysed system), and $\boldsymbol{\theta}$ is a vector of independent parameters $\boldsymbol{\theta} = (\boldsymbol{\theta}_1, ..., \boldsymbol{\theta}_n)^T$ .This implies that the ground state wave function and energy can be found by identifying the values of the parameters which minimize the energy expectation value.

As shown in Fig. 3a, the algorithms needs some information to be specified:

- **System Hamiltonian:** the Hamiltonian of the analysed problem needs to be rewritten as a qubit Hamiltonian in the from

$$H = \sum_j h_j P_j = \sum_j h_j \prod_i \sigma_j^i, \tag{4}$$

where $P_j = \sigma_1^{i_1} \otimes \sigma_2^{i_2} \otimes ...\sigma_N^{i_N}$ are the Pauli

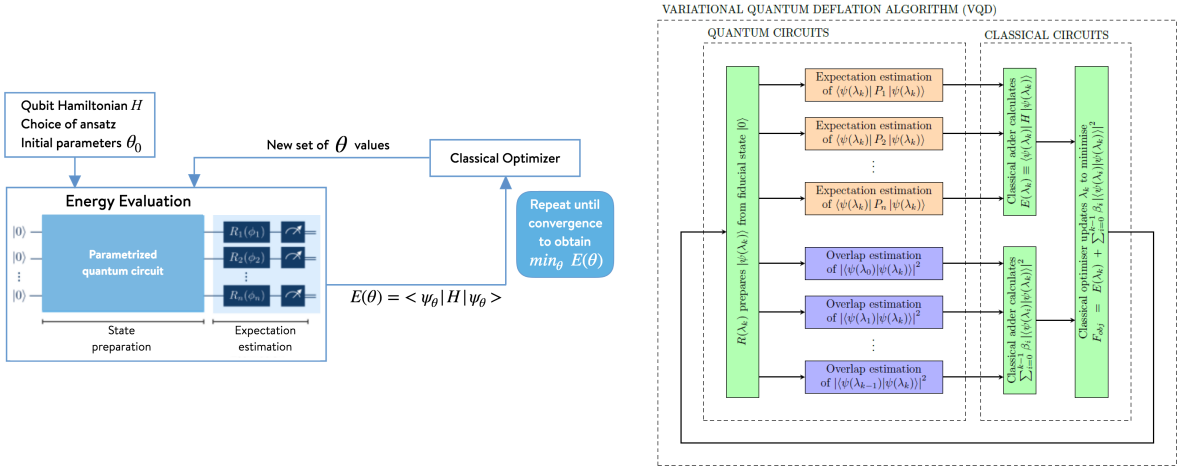

(a) VQE algorithm. (b) VQD algorithm.

Figure 3: Schematic representation of inner working of the VQE and VQD algorithms.

operators string, composed of cross product of single-qubit Pauli operators $\sigma_j^i \in \{I, X_j, Y_j, Z_j\}$ and h_j is the corresponding coefficient.

- **Variational ansatz:** this is the parameterized quantum circuit needed to prepare the state on the QPU (Quantum Processing Unit, quantum processor). It is characterized by a set of quantum gates applying parameterized rotations to the qubits $(R_x(\theta_1), R_y(\theta_2), R_z(\theta_3))$ along with fixed-angle rotations (X, Y, Z Pauli gates), Hadamard gates and entangling gates (CNOT, Toffoli). The ansatz must be engineered in order to span the Hilbert space of possible solutions.
- **Initial point:** this is the ensemble of initial parameters that can be, but not necessarily, inserted into the parameterized ansatz in order to define the initial point in the Hilbert space of possible solutions.

The algorithm starts by preparing the first version of the parameterized state on the quantum processor through the ansatz circuit. Once the trial state has been prepared, the expectation value of every Pauli operator in which the problem Hamiltonian has been decomposed (σ_j^i) needs to be evaluated. To do so, for a specified number of experiments with same parameters $|\Psi(\boldsymbol{\theta})\rangle$, each qubit's population is measured multiple times. Once these value are obtained, they are multiplied and averaged to obtain the expectation value of the Pauli strings P_j. Finally, they are multiplied by the coefficients h_j and summed to obtain the energy eigenvalue of the considered problem, the so called cost function of the VQE:

$$\begin{aligned} E(\boldsymbol{\theta}) &= \langle\Psi(\boldsymbol{\theta})|\, H\, |\Psi(\boldsymbol{\theta})\rangle \\ &= \sum_j h_j \langle\Psi(\boldsymbol{\theta})|\, P_j\, |\Psi(\boldsymbol{\theta})\rangle \end{aligned} \tag{5}$$

Once the energy is calculated on the QPU, its value is transferred to the CPU (classical processor) where optimization is performed. Here a classical optimizer evaluates how to update the set of parameters in the (quantum) ansatz to reach the lowest energy value.

3.2. Varitational Quantum Deflation (VQD) algorithm

The Variational Quantum Deflation (VQD) algorithm was first introduced in the 2019 work of Higgott et al. [7]. It is an extension of the VQE algorithm, which allows also to compute the higher excited eigenstates and eigenenergies. It consists of the same iterative procedure of the VQE algorithm comprising a state preparation phase performed on the QPU, mediated by the the ansatz circuit, followed by the energy optimization step performed on the classical CPU (see Fig. 3b). The main difference can be found in the cost function:

$$F(\boldsymbol{\theta_k}) = E(\boldsymbol{\theta}) + \sum_{i=0}^{k-1} \beta_i |\, \langle\Psi(\boldsymbol{\theta_k})|\Psi(\boldsymbol{\theta_i})\rangle\, |^2, \tag{6}$$

where k is the number of already computed eigenvalues and $E(\boldsymbol{\theta})$ is defined as in Eq. 5. This new cost function is used to minimize the parameterized energy of the k-th excited state with the constrain that the trial wavefunction $\Psi(\boldsymbol{\theta_k})$ of the currently computed excited state is orthogonal to the others $\Psi(\boldsymbol{\theta_0}), ..., \Psi(\boldsymbol{\theta_{k-1}})$. This is ensured by adding the "overlap" term $\beta_i |\langle\Psi(\boldsymbol{\theta_k})|\Psi(\boldsymbol{\theta_i})\rangle|^2$. Such term allows to exploit the fact that Hermitian matrices admit a complete set of orthogonal eigenvectors, effectively enabling the computation of the energy for the higher excited states of the system. The coefficients $\beta_1, ..., \beta_{k-1}$ (overlap weight) need to be chosen sufficiently large to ensure that the minimum value of the cost function $F(\theta_k)$ corresponds to the energy of the k-th excited state.

4. Dimer system

Dimer is a two-molecule aggregate, which has been used in this work as a test for the quantum computing performance. The single monomers (single molecule) composing it have been defined as a two level system with a ground and excited state separated by a resonance energy ϵ. When two systems of this type, described by their transition dipole, interact and couple together (see Subsec. 2.2) the excited energy spectra of the dimer system gets modified as represented in Fig. 4. In the Figure below $|G\rangle$ is a shorter notation for the ground state, $|m_1\rangle$ and $|m_2\rangle$ represent the states in which a single molecule is excited (molecule number one or two, accordingly), and $|m_{12}\rangle$ is the state with both molecules being excited.

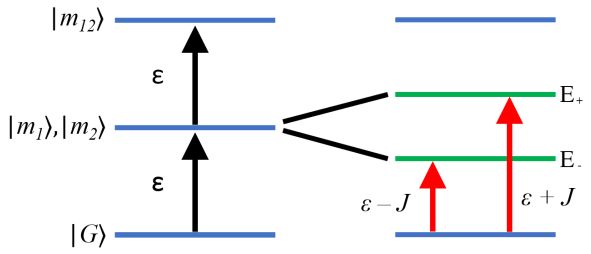

Figure 4: Coupled dimer system schematic energy spectra.

Restricting consideration to a maximum one excitation being present, the resulting Hamiltonian can be written in the following way:

$$H = \epsilon(|m_1\rangle\langle m_1| + |m_2\rangle\langle m_2|) + \\ + J(|m_1\rangle\langle m_2| + |m_2\rangle\langle m_1|) = \begin{bmatrix} \epsilon & J \\ J & \epsilon \end{bmatrix} \quad (7)$$

which eigenvalues can be easily computed analytically (see Eq. 2). Next, the Hamiltonian in Eq. 7 needs to be rewritten as the qubit Hamiltonian according to the following map:

$$\begin{aligned} |m_1\rangle\langle m_1| &\to |0\rangle\langle 0| = \frac{1}{2}(I + Z) \\ |m_2\rangle\langle m_2| &\to |1\rangle\langle 1| = \frac{1}{2}(I - Z) \\ |m_1\rangle\langle m_2| &\to |0\rangle\langle 1| = \frac{1}{2}(X + iY) \\ |m_2\rangle\langle m_1| &\to |1\rangle\langle 0| = \frac{1}{2}(X - iY) \end{aligned} \quad (8)$$

resulting in

$$H = \epsilon I + JX \quad (9)$$

where I and X are respectively the identity and x Pauli matrix. To define the parameterized ansatz, two approaches have been used: problem-agnostic (two parameterized rotations) and problem aware (one parameterized rotation), as represented in Fig. 5a and 5b respectively. While the former approach is universal and does not depend on the considered system, the latter approach takes into account the structure of the Hamiltonian (see Eq. 9), which allows to reduce the number of parameterized gates and simplify the quantum circuit.
To be specific, the TDBC fluorescent cyanine compound has been considered [8] with energy values

$$\begin{aligned} \epsilon &\approx 2.42\ eV \\ J &\approx 0.30\ eV \end{aligned} \quad (10)$$

By using these values in Eq. 2, the reference values of the two excited energy levels result,

$$\begin{aligned} E_- &= 2.12\ eV \\ E_+ &= 2.72\ eV \end{aligned} \quad (11)$$

which are used to verify the performance of the hybrid algorithms. In this work, three types of computation were exploited: a noiseless "ideal" simulator of a quantum processor (running on a classical computer), a "real" simulator of quantum processor with noise model of a real device taken into account (running on a classical

(a) Problem-agnostic ansatz. (b) Problem-aware ansatz.

Figure 5: Problem-agnostic and problem aware ansatz for the dimer system.

computer), and the real IBM quantum processor. For the simulator the "Estimator" primitive from Qiskit library, one of the two foundational building blocks for designing and optimizing quantum workloads on IBM quantum processors and simulators, has been used. Such primitive is based on the Statevector simulator which acts as an ideal quantum circuit simulator running on classical computer. For calculation on the real quantum processor, the seven-qubit Falcon r5.11H quantum processor "ibm_lagos" from IBM was chosen. For the "real" simulator, the noise model of the same processor was employed. As an example of differences in the three calculation approaches, table 1 shows the results for the Simultaneous Perturbation Stochastic Approximation (SPSA) optimizer and the problem aware-ansatz. In the graphs below (see Fig. 6), the intermediate results for the energy obtained at the end of every iteration in the VQE and VQD calculations are shown. The lines present in the graph represent the computations performed with the SPSA as well as the Constrained Optimization By Linear Approximation (COBYLA) algorithms used in the main text. Moreover, on the same graph the representation of the optimization trajectory on the Bloch sphere has been reported. The final obtained state, corresponding to the highest (for the VQD) or lowest (for the VQE) excited state is shown as a vector.

By comparing all the results obtained for the dimer system with the problem-aware ansatz (see Tab. 1) a few comments needs to be made:

- for both simulators the optimization results are coincident/close to the expected value. This is a first proof of the correct working of the developed simulation. That said a slight deviation from the analytically computed value is present for the Estimator+noise calculations as a direct cause of the noise introduced into the computation.
- The evaluation time has hugely increased after adding the noise model. This is probably due to the fact that the classical optimizers now have also to account for the noise presence, leading to an higher computational effort and a general slow down of the process.
- the results obtained with the actual quantum processor are still quite accurate for the VQE while the deviation from the expected value is pretty consistent for the VQD (more than 10%). This is probably due to the inefficiencies in the system controlling IBM quantum resources, coupled with the intrinsic errors associated with a real device. These inefficiencies and errors are also the main reasons behind the abnormal increase in evaluation time.

Calculation type	Estimator		Estimator+noise		QPU	
	VQE	VQD	VQE	VQD	VQE	VQD
Optimization result (eV)	2.1200	2.7200	2.1317	2.7159	2.1260	3.0633
Evaluation time (s)	0.456	1.299	23.345	53.429	3198	20633
Deviation from expected value (%)	0	0	0.55	0.15	0.28	12.62
Iterations	171	251	171	251	171	251

Table 1: Results of dimer system VQE and VQD calculations with problem-aware ansatz for Estimator primitive, Estimator plus real device noise model and real QPU. Values are only for SPSA optimizer.

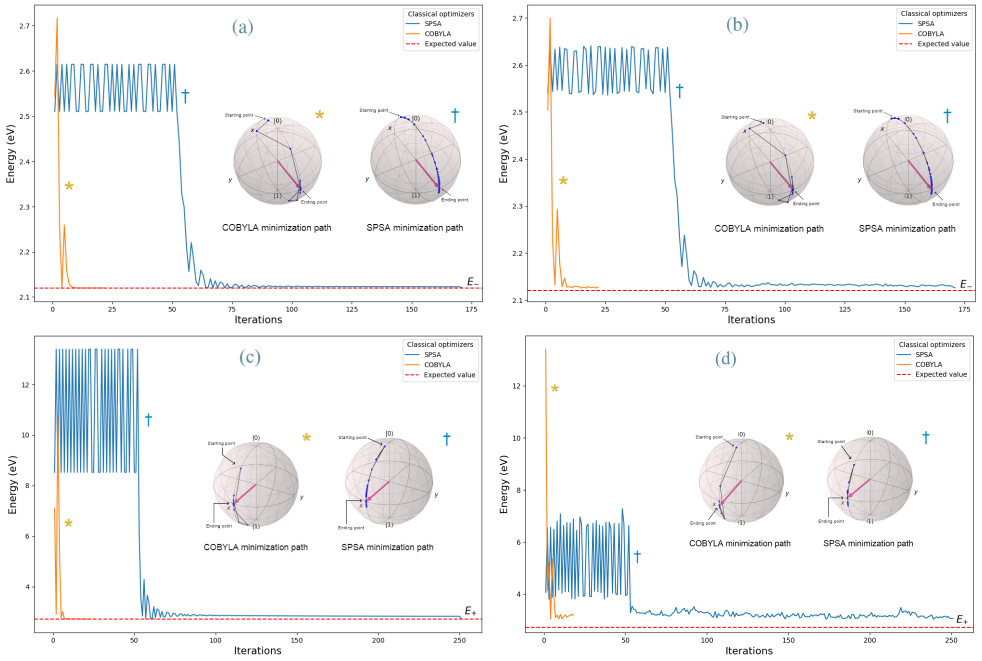

Figure 6: Intermediate steps graphs for VQE (a-b) and VQD (c-d) calculations with problem-aware ansatz for Estimator primitive (a-c) and real QPU (b-d).

5. Tetramer system

The developed methodology for computing the excited energy spectra has then been tested on a more complex system, the tetramer (four molecules system). First of all, as for the dimer case, also for this system the system Hamiltonian has been defined. The employed model was drawn directly from the one used in paragraph 4. This means the four molecules have been modelled as two levels systems with a ground and excited state separated by a resonance energy ϵ. When the transition dipole moment associated to the exciton of a monomer couples with the others, the excited energy spectra of the tetramer gets modified as shown in Fig. 7. In the same picture $|G\rangle$ represents again the ground state, whereas $|m_1\rangle$, $|m_2\rangle$, $|m_3\rangle$ and $|m_4\rangle$ represent respectively the states in which a single molecule between the four is excited

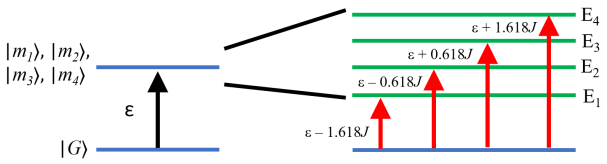

Figure 7: Coupled tetramer system schematic energy spectra.

The resulting Hamiltonian for the excited energy levels of the described system is the follow-

ing

$$H = \begin{bmatrix} \epsilon & J & 0 & 0 \\ J & \epsilon & J & 0 \\ 0 & J & \epsilon & J \\ 0 & 0 & J & \epsilon \end{bmatrix} \tag{12}$$

Where ϵ is the excited energy of the single monomer and J is the exciton slitting term described, in accordance with the point-dipole approximation as a Coulomb interaction. Also for this system the eigenvalue can easily be compute analytically and are equal to

$$\begin{aligned} E_1 &= \epsilon - \frac{1+\sqrt{5}}{2} J \approx \epsilon - 1.618J \\ E_2 &= \epsilon + \frac{1-\sqrt{5}}{2} J \approx \epsilon - 0.618J \\ E_3 &= \epsilon - \frac{1-\sqrt{5}}{2} J \approx \epsilon + 0.618J \\ E_4 &= \epsilon + \frac{1+\sqrt{5}}{2} J \approx \epsilon + 1.618J \end{aligned} \tag{13}$$

The Hamiltonian in Eq. 12 has then been mapped into the qubit base thanks to equivalences similar to the one in Eq. 8, but adapted to a larger 2×2 matrix. The resulting Hamiltonian in the qubit base is expressed by the following sum of Pauli matrices products

$$\begin{aligned} H = \epsilon\ I_{q1}I_{q2} + J[I_{q1}X_{q2} + \\ + 0.5(X_{q1}X_{q2} + Y_{q1}Y_{q2})] \end{aligned} \tag{14}$$

where I is the identity matrix, whereas X and Y respectively the x and y Pauli matrices. The subscripts $q1$ and $q2$ refer to the qubits which compose the ansatz quantum circuit and to which the Pauli matrices are referred to. For what concerns the chosen ansatz circuit they have been defined by employing the Schmidt decomposition and Singular Value Decomposition theorem. The resulting circuits were divided in two problem-agnostic ansatz with nine and six parameters respectively and a problem-aware ansatz with three parameters. For the numeric values of ϵ and J the numbers shown in Eq. 10 have been again considered. By inserting them in Eq. 13 the resulting expected values for the excited energy spectra are

$$\begin{aligned} E_1 &\approx 1.9346\ eV \\ E_2 &\approx 2.2346\ eV \\ E_3 &\approx 2.6054\ eV \\ E_4 &\approx 2.9054\ eV \end{aligned} \tag{15}$$

which could be used to benchmark the results of the hybrid algorithms and verify their accuracy also for the tetramer system. The computations have been performed again with the noiseless simulator Estimator primitive and with the simulator provided of the real device "ibm_lagos" noise model. It has not been possible to perform the computation for the tetramer system on the real quantum processor due to the fact that they exceeded the maximum allowed time limit for computation on IBM devices. By looking at the obtained results (see Tab. 2), which for brevity have been limited to the SPSA optimizer only, also for the tetramer problem some observations can be made:

- the obtained results for the tetramer system required much more iterations and evaluation time time compared to the dimer one (Tab. 1). This is a direct consequence of the increased size of the system which inevitably leads to an increased computational effort for both the state preparation phase (due to more parameters) as well as the classical optimizer step (due to more parameters as well as more noise to handle).
- The deviation from the expected value for the VQD results is not negligible being it more than 5% for the Estimator primitive results. This is again related to the increase size of the system and the increased complexity of the analysed cost-function with respect to the VQE one.
- In line with what happened for the dimer system, also for the tetramer one the introduction of noise in the system leads to a huge increase in computational time mostly related to the higher computational burden that the noise exercise on the classical optimizers

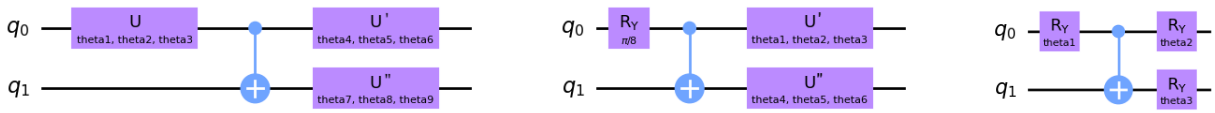

(a) Problem-agnostic ansatz with 9 parameters. (b) Problem-agnostic ansatz with 6 parameters (c) Problem-aware ansatz with 3 parameters.

Figure 8: Problem-agnostic and problem aware ansatz for the tetramer system.

	Estimator		Estimator+noise	
Calculation type	**VQE**	**VQD**	**VQE**	**VQD**
Optimization result (eV)	1.9346	2.4057 2.5987 2.7388	1.9512	2.2718 2.5882 2.8783
Evaluation time (s)	2.059	29.99 40.40 33.49	524	1341 1077 1077
Deviation from expected value (%)	0	7.66 0.26 5.73	0.85	1.66 0.66 0.93
Iterations	851	4051 4051 4051	2051	35 45 45

Table 2: Results of tetramer system VQE and VQD calculations with problem-aware ansatz for Estimator primitive and Estimator plus real device noise model. Values are only for SPSA optimizer.

6. Conclusions

The aim of this work has been to evaluate whether or not quantum computers employing hybrid quantum-classical algorithms could be used to effectively simulate molecular aggregate excited energy spectra. While the developed method allowed to compute the desired observables for the two small systems dimer and tetramer, computational times and deviation from expected value were not exactly optimal. This can be traced back to multiple reasons starting from the inefficiencies in the infrastructure managing the quantum resources, which leads to computational times of thirty seconds per iteration versus milliseconds on classical devices, the intrinsic error inducing noise characteristic of NISQ devices and the iterative nature of VQE and VQD algorithms. In order to obtain a quantum advantage (meaning an exponential speed-up on the same task performed with classical computers) full Quantum Error Correction (QEC) needs to be achieved in order to implement Fault-Tolerant Quantum Computing and overcome the shortcomings of current devices. Moreover, some other future developments on the defined method are worth mentioning:

- the fidelity and accuracy of the simulation could be increased by respectively adding off-diagonal elements and deviations from ideality into the system Hamiltonian (Eq. 12) and introducing error mitigation techniques into the computations.
- The simulation could be made fully quantum by employing instead of VQE and VQD, the Quantum Phase Estimation algorithm. This algorithm allows high precision measurements of ground and excited state energies. To perform such task it starts by preparing a trial initial state which is then evolved through a quantum circuit into a superposition of time evolved states over a suitable range of evolution times t. Another method could also be the simulation of the system in a analogue fashion. This would entail building a quantum chip with engineered interactions between the qubits in

order to map its Hamiltonian onto the one of the molecular aggregate system. Both these techniques are nowadays hindered by the limited resources of NISQ devices.

References

[1] M. A. Nielsen and I. L. Chuang, *Quantum Computation and Quantum Information*. Cambridge University Press, New York, 2010.

[2] A. N. Vetlugin, C. Soci, and N. I. Zheludev, "Modelling quantum photonics with a transmon of the ibm quantum computer," *Appl. Phys. Lett. 121*, pp. 1–6, 2022.

[3] S. McArdle, S. Endo, A. Aspuru-Guzik, S. C. Benjamin, and X. Yuan, "Quantum computational chemistry," *Rev. Mod. Phys.*, p. 015003, 2020.

[4] M. Kasha, H. R. Rawls, and M. A. El-Bayoumi, "The exciton model in molecular spectroscopy," *Pure and Applied Chemistry, vol. 11, no. 3-4*, pp. 371–392, 1965.

[5] J. Frenkel, "On the transformation of light into heat in solids. i," *Nature 138*, pp. 17–44, 1931.

[6] A. Peruzzo, J. McClean, and P. e. a. Shadbolt, "A variational eigenvalue solver on a photonic quantum processor," *Nat Commun 5, 4213*, pp. 1–7, 2014.

[7] O. Higgott, D. Wang, and S. Brierley, "Variational quantum computation of excited states," *Quantum 3, 156 (2019)*, pp. 1–11, 2019.

[8] K. S. Semion, A. Eisfeld, S. Valleau, and A. Aspuru-Guzik, "Photonics meets excitonics: natural and artificial molecular aggregates," *Nanophotonics, vol. 2, no. 1*, pp. 21–38, 2013.